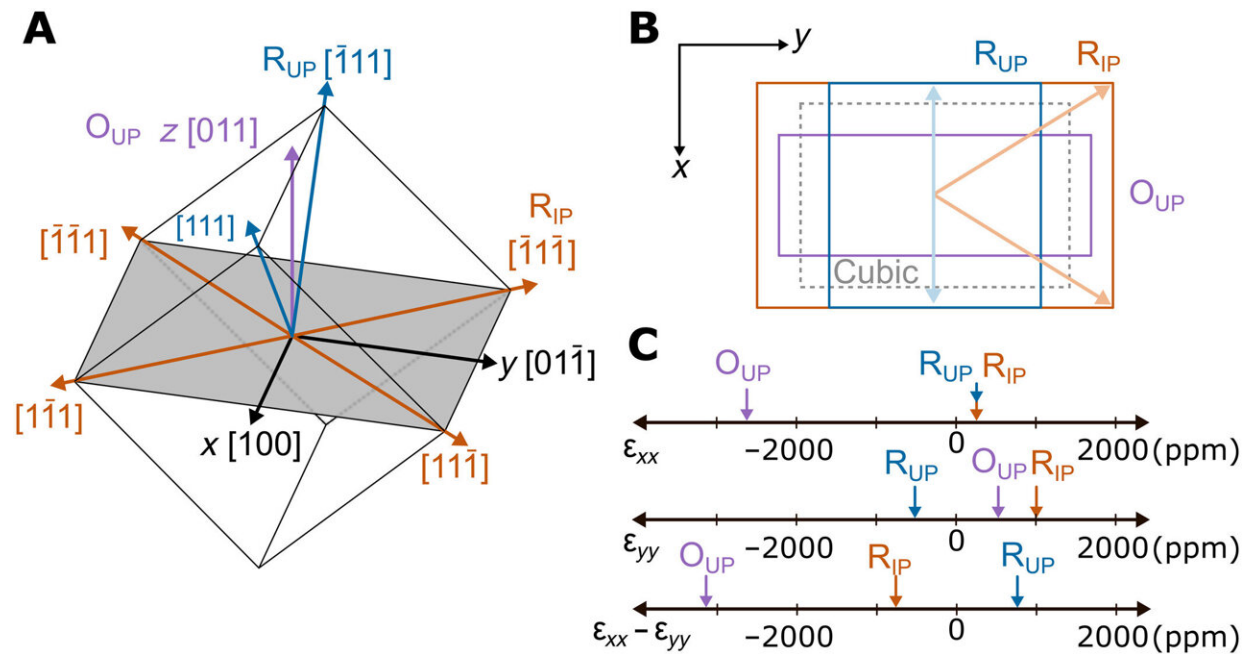


# Low-voltage magnetoelectric coupling in membrane heterostructures

November 19 2021, by Thamarasee Jeewandara



Anisotropic strain in (011)-oriented PMN-PT. (A) Cartesian coordinates  $x$ ,  $y$ , and  $z$  are defined to be the crystal  $[100]$ ,  $[011^-]$ , and  $[011]$  directions, respectively. Polarization directions in (011)-oriented PMN-PT unit cell, grouped into rhombohedral in-plane (RIP; orange), rhombohedral up (RUP; blue), and orthorhombic up (OUP; purple). Rhombohedral down (RDOWN) and orthorhombic down (ODOWN) are not shown but are, respectively, RUP and OUP mirrored about the  $xy$  plane. The in-plane cut through the unit cell (shaded gray area) is rectangular with sides of length  $a\sqrt{2}$  by  $a$ , where  $a$  is the lattice parameter. (B) Electrostrictive deformations (not to scale) of the unit cell for the cubic (zero FE polarization), RIP, RUP, and OUP polarization groups. The down deformations are identical to up. In-plane projections of polarization vectors are shown for RIP (light orange) and RUP (light blue). (C) Plots of linear

electrostriction strains  $\epsilon_{xx}$  and  $\epsilon_{yy}$  and the anisotropic strain  $\epsilon_{xx} - \epsilon_{yy}$  for RIP, RUP, and OUP polarization groups. Credit: Science Advances, 10.1126/sciadv.abh2294

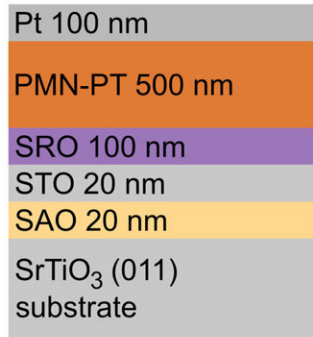
Strain-mediated magnetic coupling in ferroelectric and ferromagnetic heterostructures can offer a unique opportunity for scientific research in low-power multifunctional devices. Ferroelectrics are materials that can maintain spontaneous and reversible electric polarization. Relaxor-ferroelectrics that exhibit high electrostriction are ideal candidates for ferroelectric layer constructs due to their large piezoelectricity. Although the properties of relaxor ferroelectrics are known, their mechanistic origins remain a mystery, giving rise to an enigmatic form of materials. In addition to that, thin films are ineffective from [substrate clamping](#) and can substantially reduce piezoelectric in-plane strains. In a new report now published in *Science Advances*, Shane Lindemann and a research team in materials science, and physics in the U.S. and Korea, displayed low-voltage magnetoelectric coupling in an all-thin-film heterostructure using anisotropic strains induced by the orientation of the material. The team used an ideal ferroelectric layer of  $\text{Pb}(\text{Mg}_{1/3}\text{Nb}_{2/3})\text{O}_3\text{-PbTiO}_3$  abbreviated [PMN-PT](#) during this work and coupled it with ferromagnetic nickel overlayers to create membrane heterostructures with magnetization. Using scanning transmission electron microscopy and phase-field simulations, they clarified the membrane response to understand the microstructural behavior of PMN-PT thin films, to then employ them in piezo-driven magnetoelectric heterostructures.

## Magnetoelectric (ME) coupling

The electric field control of magnetism also known as converse [magnetoelectric coupling](#) has potential for next-generation memory

storage and sensing technologies. The PMN-PT material is of interest as a relaxor-ferroelectrics material for applications as the ferroelectric layer with a large piezoelectric composition. By coupling the relaxor-ferroelectric with a ferromagnet containing large magnetostriction, converse ME coupling can be achieved by transferring voltage-induced strain from the ferroelectric layer in to the ferromagnetic layer to result in the strain-mediated control of [in-plane anisotropy](#), tunneling magnetoresistance, [ferromagnetic resonance](#) and [conductivity](#). The recent drive towards low-power ME devices and the development of micro- and nanoelectromechanical systems has led to further study of relaxor-ferroelectric thin [films](#). Reducing the thin-film dimensions of relaxor-ferroelectrics can induce a large reduction in piezoelectricity due to mechanical clamping, and scientists therefore aim to overcome this challenge successfully to integrate relaxor-ferroelectric thin films into high-performance devices. In this work, Lindemann et al. overcame the clamping issue and demonstrated low-voltage strain-mediated ME coupling in all-thin-film heterostructures. The work highlighted the microscopic nature of relaxor-ferroelectric thin films to present a crucial step toward their applications in low-power piezo-driven magnetoelectric devices.

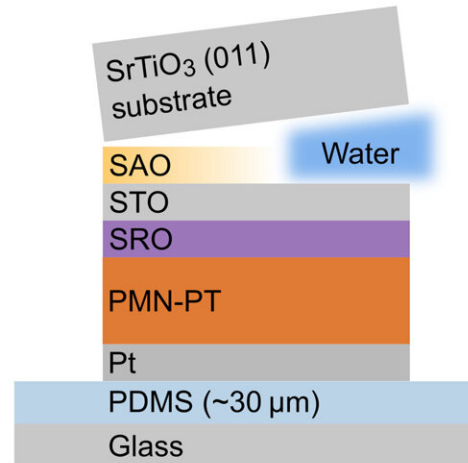
**A** Initial heterostructure



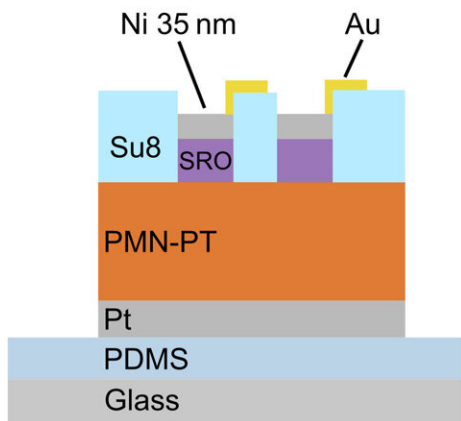
Flip over

Attach to PDMS/glass

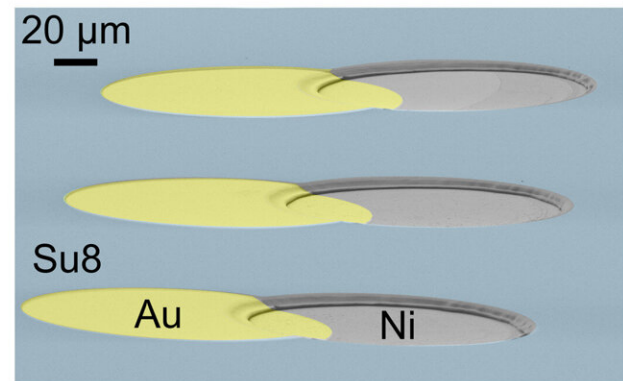
**B** Water etching of sacrificial SAO layer



**C** Deposit Ni  
Pattern Ni/SRO into discs  
Add Au/Su8



**D** SEM of final heterostructure



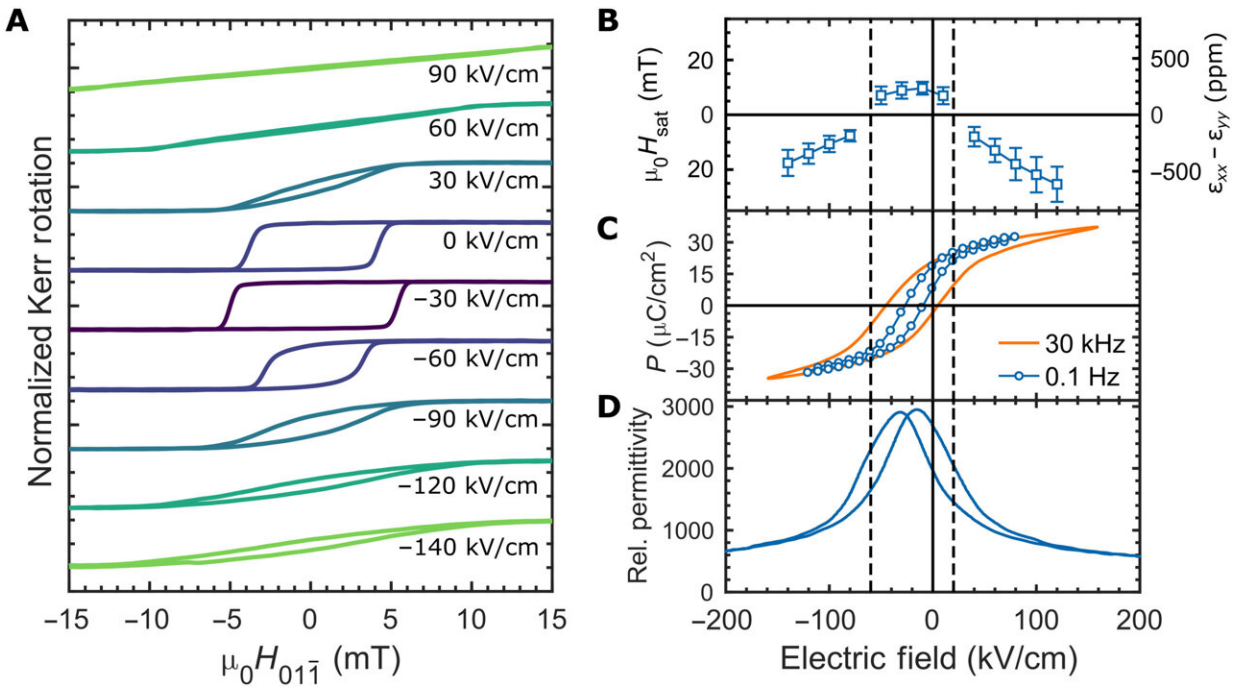
Fabrication of single-crystal (011)-oriented PMN-PT membrane heterostructures. (A) Initial thin-film heterostructure consisting of PLD-grown SAO/STO layers and sputter-deposited SRO/PMN-PT/Pt layers. (B) After attaching the heterostructure Pt-side into PDMS/Glass, the SAO sacrificial layer is etched by H<sub>2</sub>O. (C) After removal of the STO buffer layer, Ni is deposited by sputtering followed by patterning of the Ni/SRO layers into 160- $\mu$ m circles. The membrane heterostructure is completed by addition of the SU-8 protective layer and Au-lifted electrode layer. (D) SEM image showing the completed membrane device. Credit: Science Advances, 10.1126/sciadv.abh2294

## Developing and characterizing membrane heterostructures

Lindemann et al. measured the strain-induced changes of magnetic anisotropy in the nickel overlayer using longitudinal [magneto-optic Kerr effect](#) (MOKE) hysteresis loops, as a function of PMN-PT bias electric fields. They then showed the significance of removing mechanical clamping by the substrate to achieve large anisotropic in-plane strains. To then understand the strain behavior inferred from the magneto-optic Kerr effect hysteresis, Lindeman et al. plotted the calculated magnetic anisotropy energy density, determined from the saturation field of hard axis loops, and the known differential strain based on the known magnetostriction of nickel. They then determined the domain structure of the as-grown PMN-PT membranes using [scanning transmission electron microscopy](#). The single-crystalline material showed a columnar structure with lattice mismatch during the growth of the film. The findings resembled a mixed ferroelectric and relaxor domain structure consistent [with the experimental model](#).

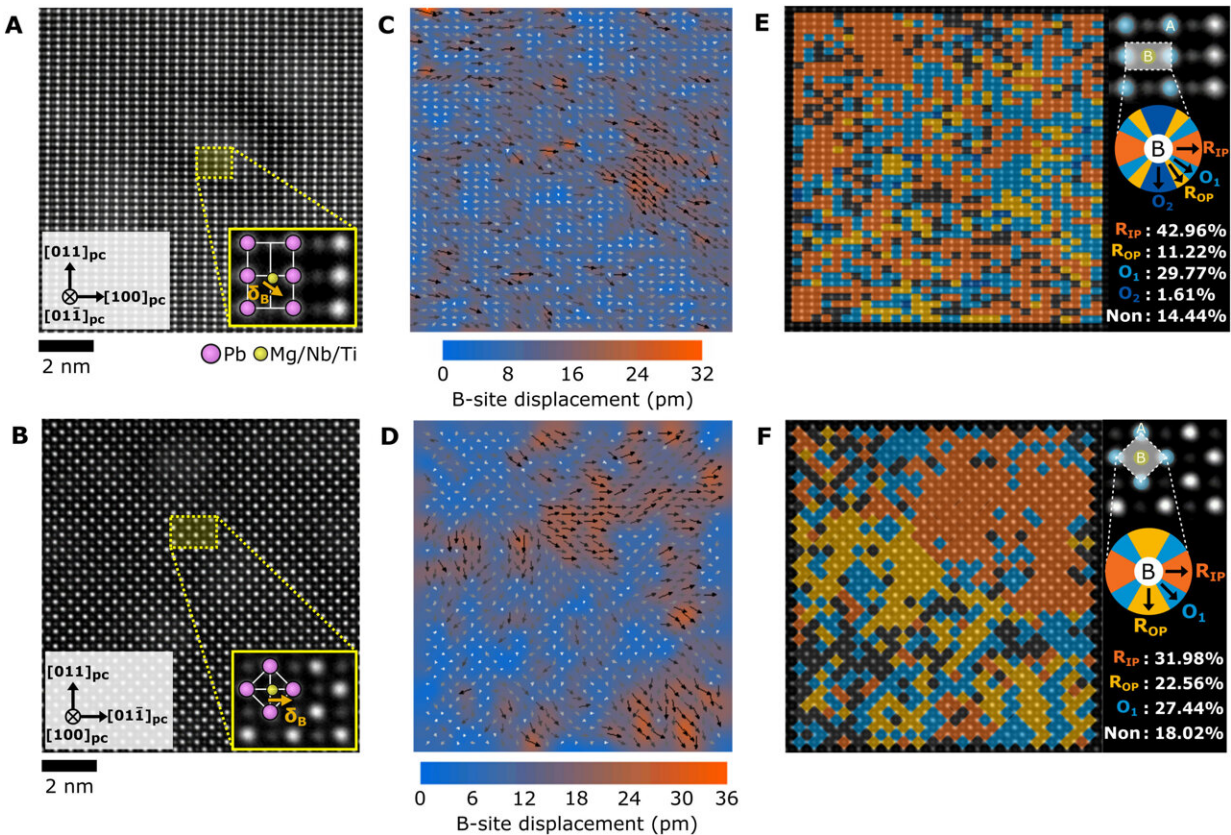
## Phase-field simulations of PMN-PT membranes

To then understand the strain behavior of the PMN-PT membrane, the scientists next performed phase-field simulations. To measure the average strain, they calculated the strain contribution of individual spontaneous polarization elements, multiplied by the electrostriction tensor. The starting point of the simulation indicated the expected structure around the ferroelectric imprint of the experimental PMN-PT membrane. The results of the simulation qualitatively agreed with the experimental strain and polarizations measured in the PMN-PT/nickel membrane. While the strains calculated from the experimental MOKE ([magneto-optic Kerr effect](#)) loops exhibited a horizontal and vertical shift relative to the calculated strains from simulation, qualitatively, the two curves were similar.

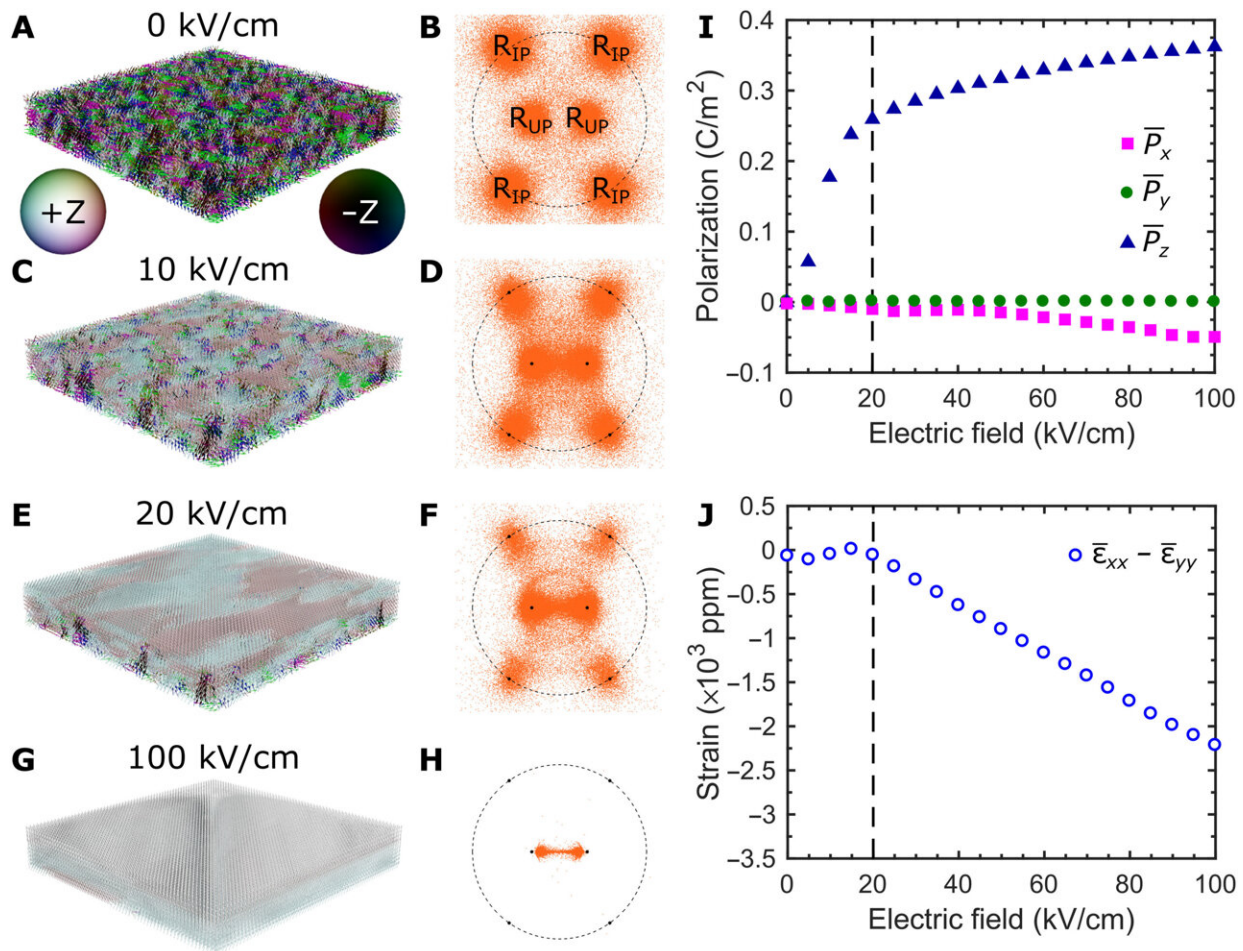


Magnetolectric (ME), ferroelectric (FE), and piezoelectric properties of PMN-PT membrane heterostructures. (A) MOKE magnetic hysteresis loops (normalized) at a series of electric fields from  $-140$  kV/cm ( $-7$  V) to  $90$  kV/cm ( $4.5$  V). Dark colors are closer to the FE imprint, and lighter colors are further from the imprint. (B) Saturation magnetic field ( $H_{\text{sat}}$ ; left axis) and calculated anisotropic strain ( $\epsilon_{xx} - \epsilon_{yy}$ ; right axis) versus biasing electric field extracted from HA MOKE hysteresis loops similar to those shown at high-bias electric field in (A). Error bars represent the SD of measurements of seven different devices on the same membrane. Negative differential strain points ( $\epsilon_{xx} - \epsilon_{yy} < 0$ ) from loops where magnetic field was along  $[100]$ . (C) Polarization ( $P$ ) vs electric field hysteresis loop measurements using the  $160\text{-}\mu\text{m}$ -diameter Ni/SRO top electrode. The orange loop was measured with a  $30\text{-kHz}$  sinusoidal voltage pulse. The blue curve, labeled as  $0.1$  Hz, was acquired using a quasi-DC measurement procedure (see Methods). (D) Relative permittivity versus biasing electric field. Bias electric field was swept at  $0.5$  Hz, and permittivity was measured with a small AC electric field of  $3.5$  kV/cm RMS at  $4$  kHz. For (B) to (D), guidelines are added to separate the behavior into a low-field region (near FE imprint) and high-field regions. Credit: Science Advances, 10.1126/sciadv.abh2294





STEM analysis of domains present in the PMN-PT membrane. (A and B) Atomic resolution high-angle annular dark-field (HAADF)–STEM images along the  $[011]_{pc}$  and  $[100]_{pc}$  zone axes, respectively. The insets are enlarged images in each zone axis. Pink circles are A-site cations (Pb) and yellow circles are B-site cations (Mg/Nb/Ti). Orange arrows are the B-site displacement ( $\delta_B$ ). (C and D) B-site cation displacement mapping with overlaid arrows indicating regions of short-range ordering. Color maps show the atomic displacement magnitude, and arrows display the direction of atomic displacement. (E and F) Phase fraction mapping in each unit cell with color wheel by expected B-site displacement directions for RIP (R1), ROP (R2), and regions that have displacements between the R states labeled as orthorhombic O1 and O2. Color blank regions (Non) indicate the nonpolar region under the 7 pm of B-site displacement. Credit: Science Advances, 10.1126/sciadv.abh2294



Phase-field simulations of the (011) PMN-PT membrane. Spontaneous polarization and [011] stereographic projection of the PMN-PT membrane at (A and B) 0 kV/cm, (C and D) 10 kV/cm, (E and F) 20 kV/cm, and (G and H) 100 kV/cm. The legend for the coloring of spontaneous polarization is included in (A). (I) Average polarization in the x, y, and z directions versus applied field. (J) Field dependence of the average anisotropic in-plane strain  $\bar{\epsilon}_{xx} - \bar{\epsilon}_{yy}$ . In (I) and (J), guidelines have been added to separate the low-field and high-field regions. Credit: Science Advances, 10.1126/sciadv.abh2294

## Outlook



In this way, Shane Lindemann and colleagues showed the low-voltage, strain-mediated, magnetoelectric (ME) effect in an all-thin-film heterostructure. The film only relied on the large anisotropic [strains](#) inherent to the PMN-PT [thin films](#). The PMN-PT/nickel membrane used in this work achieved a robust, piezo-driven, 90 degree rotation of the in-plane magnetic anisotropy of the nickel overlayer under a small voltage of bias to result in strain anisotropy, controlled by the in-plane crystal symmetry of the PMN-PT film. Using scanning [transmission electron microscopy](#), the scientists showed the microscopic structure of the PMN-PT [membrane](#). Then using bulk PMN-PT, they showed how the material exhibited permanent switching between in-plane and out-of-plane polarization states; this behavior provided a desirable trait for memory storage. The work provides key insight to the microstructural behavior of PMN-PT thin film membranes to show their applications in magnetoelectric coupling devices, and also predict their use with a variety of other materials to discover previously unknown piezo-driven phenomena.

**More information:** Shane Lindemann et al, Low-voltage magnetoelectric coupling in membrane heterostructures, *Science Advances* (2021). [DOI: 10.1126/sciadv.abh2294](https://doi.org/10.1126/sciadv.abh2294)

Sasikanth Manipatruni et al, Scalable energy-efficient magnetoelectric spin-orbit logic, *Nature* (2018). [DOI: 10.1038/s41586-018-0770-2](https://doi.org/10.1038/s41586-018-0770-2)

© 2021 Science X Network

Citation: Low-voltage magnetoelectric coupling in membrane heterostructures (2021, November 19) retrieved 21 June 2024 from <https://phys.org/news/2021-11-low-voltage-magnetoelectric-coupling-membrane-heterostructures.html>

This document is subject to copyright. Apart from any fair dealing for the purpose of private

study or research, no part may be reproduced without the written permission. The content is provided for information purposes only.